

Observing the APOD Satellite with the AuScope VLBI Network

Andreas Hellerschmied¹, Lucia McCallum², Jamie McCallum², Johannes Böhm¹, Jing Sun³

Abstract The Chinese APOD-A nano satellite, launched in September 2015, is the first LEO satellite co-locating three space-geodetic techniques including VLBI. Being equipped with a dual-frequency GNSS receiver, an SLR retro-reflector, and a VLBI beacon transmitting DOR tones in the S- and X-band, it can be considered as a first prototype of a geodetic co-location satellite in space. With the focus on VLBI observations we present a series of experiments carried out by the AuScope geodetic VLBI array in November 2016. These experiments represent first observations of a LEO satellite by VLBI radio telescopes with the goal of deriving baseline delays as common in the geodetic VLBI. In this paper we give an overview on the applied process chain that covers all tasks and aspects from scheduling and observations, over correlation and fringe fitting, to the actual data analysis. To stay as close as possible to the operational analysis scheme for geodetic VLBI sessions, we widely adopted the use of standard software such as DiFX for correlation and the Haystack Observatory Post-Processing System (HOPS). In the subsequent analysis of the derived delays in the Vienna VLBI and Satellite Software (VieVS) we find residuals in the range of a few nanoseconds. VieVS provides options to estimate a variety of geodetic parameters based on such data, including orbit offsets. The discussed experiments represent the first end-to-end realizations of VLBI observations of a tie satellite on a LEO orbit and are a valuable resource for future, more sophisticated space tie satellite missions in the style of E-GRASP/Eratosthenes.

Keywords APOD, VLBI satellite tracking, AuScope

1 Introduction

The co-location of space-geodetic techniques (including VLBI) on Earth-orbiting satellites bears promising prospects regarding inter-technique ties. For example, observations of a satellite equipped with SLR, DORIS, VLBI, and GNSS capabilities would enable establishing technique ties in space, supplementary to the local ties at co-location sites on the ground used for the ITRF combination (e.g. Altamimi et al., 2016). Such an approach was followed by two major satellite missions, GRASP (Nerem and Draper, 2011) and E-GRASP/Eratosthenes (Biancale et al., 2017), which were proposed to NASA and ESA, respectively. Although their scientific significance was recognized, both missions were eventually not approved.

Contrary to the SLR, DORIS, and GNSS, which are routinely applied for satellite tracking, observations of satellites with geodetic VLBI systems (aiming at deriving observables in terms of group delays) are non-standard. Hence, suitable tracking and data processing schemes are still a matter of research. Over the past years different groups worked on improved satellite observation capabilities of VLBI and reported on successful tracking experiments. However, due to the lack of suitable targets for VLBI, mostly GNSS satellites were observed in the L-band, e.g. Plank et al. (2017), Hellerschmied et al. (2014), Tornatore et al. (2014), and Haas et al. (2017).

The first opportunity for carrying out satellite observations in the S- and X-band, which are routinely observed by geodetic VLBI and compatible to stan-

1. Technische Universität Wien, Austria

2. University of Tasmania, Australia

3. National Astronomic Observatory, China

standard receiver equipment, was provided by the Chinese APOD-A nano satellite (hereinafter abbreviated as APOD). As described in Section 2, APOD can be considered as a first prototype of a co-location satellite in a low Earth orbit (LEO) including VLBI capabilities. In this paper we describe the only coordinated series of VLBI observations of APOD which was observed in November 2016 by the AuScope geodetic VLBI array (Lovell et al., 2013). The goal of this case study was to derive observables in terms of group delays — as is common in geodetic VLBI — based on observations of satellite signals and by applying standard observation and data processing schemes as far as possible. This proceedings contribution is a summary of a more detailed paper by Hellerschmied et al. (2018).

2 The APOD-A Nano Satellite

APOD-A nano is a Chinese cube satellite launched in September 2015 and controlled by the Beijing Aerospace Control Center (BACC). It orbits the Earth in a circular near-polar orbit with an inclination of about 97° . At the time the described observations were carried out the orbit altitude was about 450 km. The geodetic payload consists of a dual frequency GNSS receiver (capable of processing GPS and Beidou signals), an SLR retro-reflector, and a VLBI beacon emitting narrow-bandwidth DOR tones in the S- and X-band.

The structure of the VLBI signal in the S- and X-band is indicated in Figure 2. In both bands a carrier tone (long black lines) is symmetrically surrounded by four DOR tones (short black lines), yielding a total frequency span of 10.3 MHz in the S- and 38.3 MHz in the X-band.

Unfortunately, the on-board GNSS receiver which is used for the precise orbit determination (POD) by BACC partly failed in January 2016. Consequently, the accuracy of the final orbit solution (used for the calculation of theoretical near-field delays, required for the correlation and data analysis) dropped from the initial level of a few cm to the level of 10 to 20 m. Also, the orbit predictions used for tracking APOD with the AuScope antennas showed uncertainties of up to 1 km. These circumstances had wide-ranging consequences at different stages of this study.

More details about the APOD mission, the payload, the VLBI signal, and the POD are discussed by Sun et al. (2018).

3 Experiments

Table 1 APOD sessions observed in November 2016 by AuScope. The session durations and the experiment codes are listed in columns two and three, respectively.

Date	Duration	Exp. code	Stations	Targets
11.11.2016	33 min	316a	Ke, Yg	APOD, quasars
12.11.2016	41 min	317a	Ke, Hb	APOD, quasars
12.11.2016	35 min	317b	Ke, Yg, Hb	APOD, quasars
13.11.2016	26 min	318b	Ke, Yg, Hb	APOD, quasars
13.11.2016	26 min	318c	Ke, Hb	APOD, quasars
13.11.2016	23 min	318d	Ke, Yg	APOD, quasars
14.11.2016	40 min	319a	Ke, Yg, Hb	APOD, quasars
27.11.2016	24 h	a332	Ke, Yg, Hb	APOD, quasars

APOD was tracked by the three AuScope antennas — HOBART12 (Hb), KATH12M (Ke), and YARRA12M (Yg) — whenever there was common visibility by two antennas from November 11 to 14, 2016, yielding in total seven short sessions with durations of about 30 minutes (see Table 1). Throughout these sessions, first a block of about five strong quasars was observed, followed by one to two APOD tracks, and then again a block of quasars. The quasar observations were used to check the signal chains and to calculate the initial clock model for the correlation. Experiment a332 basically represents a geodetic 24-hour session with 761 scans of strong quasars (min. 0.65 Jy), intersected by four APOD scans.

3.1 Scheduling and Observations

All observations were planned by using a dedicated satellite scheduling program (Hellerschmied et al., 2017) which is implemented as a module in the Vienna VLBI and Satellite Software (VieVS; Böhm et al., 2018). VieVS generated VEX-formatted schedule files for controlling the receivers and the subsequent correlation process. Furthermore, VieVS was used to write tracking files containing azimuth and elevation positions of APOD in one second intervals, calculated

based on orbit predictions by BACC. These tracking files could be directly loaded by the AuScope antenna control units and enabled to track the fast moving LEO satellite continuously while data was recorded.

The experiment design was mainly determined by continental-wide baselines (between 2,360 and 3,432 km, see Figure 1) and the very low orbit of APOD (about 450 km), which significantly limited common visibility of the target. Hence, this observation geometry only enabled observing of single baseline scans during one to three overpasses per day. The situation is shown in Figure 1 for the Scans 168 and 169 in Experiment a332. APOD crossed Australia in the North-South (or vice versa) direction and was first observed on the baseline Hb-Yg for about 1.5 minutes (Scan 168), followed by a second scan on the baseline Yg-Ke (about a five minute duration). These two scans serve as a generic example for all further discussions in this paper.

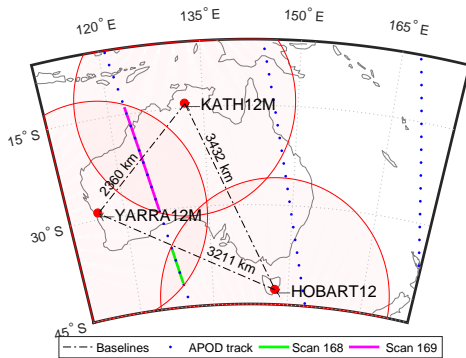


Fig. 1 Observation geometry in session a332. The antennas’ projected fields of views are indicated by red circles. From Hellerschmied et al. (2018).

The observation mode aimed at goals: (1) to capture all APOD tones and (2) to allow the computation of reasonable multiband delays (MBD) based on observations of natural radio sources. For (2) a broad frequency span is needed. Hence, in total 16 16 MHz channels were recorded — six in the S- and ten in the X-band as indicated in Figure 2. All S-band tones of the APOD signal were recorded within one 16 MHz channel, whereas three channels were needed to record all X-band tones. A 2-bit sampling was used yielding a data rate of 64 Mbps per channel.

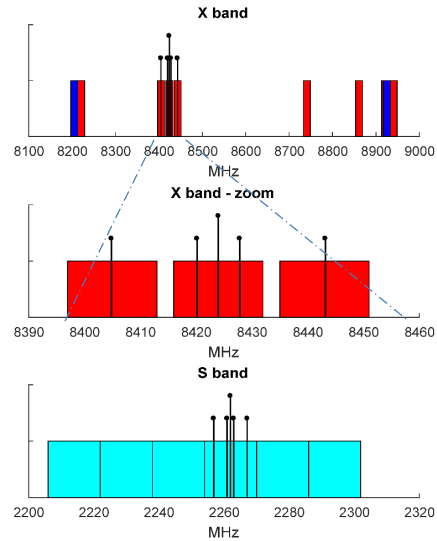


Fig. 2 Observation mode using ten 16 MHz channels in the X- and six in the S-band. APOD tones are indicated by black lines.

4 Correlation and Fringe Fitting

The recorded data was correlated with DiFX 2.5 (Deller et al., 2011) on the Vienna Scientific Cluster (VSC-3)¹. For processing the APOD observations, the standard a priori delay model was replaced by a dedicated near-field delay model calculated in VieVS based on the final orbit solution by BACC. 32 kHz wide zoom bands centered on the DOR and carrier tones were used to extract the APOD signals from the recorded 16 MHz channels.

In the next step HOPS/fourfit² was used to calculate MBDs based on the correlated zoom band channels in the S- and X-band. We found smooth residual delays for both frequency bands in a range of typically ± 10 ns. The SNR is in general extremely high with values typically between 200 and 800.

5 Data Analysis

In order to mitigate the effects of the ionosphere, the ionosphere-free linear combination of the S- and X-band MBDs was calculated according to Alizadeh et al. (2013). In a first step, these values were ana-

¹ <http://vsc.ac.at/systems/vsc-3/>

² <https://www.haystack.mit.edu/tech/vlbi/hops.html>

lyzed in VieVS by investigating the observed minus computed (OMC) residuals. The theoretical delays were computed by applying the near-field delay model by Klioner (1991) and the VieVS default setup for geophysical modeling. Typically, the OMC residuals are on a level of about 10 ns. An example for two consecutive APOD scans is depicted in Figure 3. Investigations showed that the clear systematic signature (bent shape) can mostly be explained by an along-track offset in the orbit data which was used for modeling the computed delays. Taking into account the fact that the available orbit data is only accurate on the level of about 10 to 20 m, we concluded that it is mandatory to estimate orbit parameters. Otherwise, unmodeled orbit errors would propagate into other target estimates.

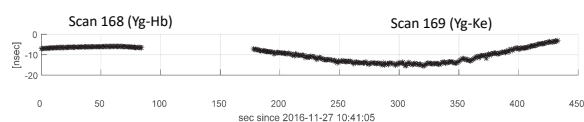


Fig. 3 Observed minus computed residuals of Scans 168 and 169 in Experiment a332.

In a simple test case, we estimated constant offsets for station clocks (Yg is the reference), zenith wet delays (ZWD), and the satellite orbit (three components) based on the OMC residuals plotted in Figure 3. The estimation results are shown in Table 2, and the post-fit residuals (WRMS of 9.5 cm) are depicted in Figure 4. Considering the rather non-ideal circumstances (weak observation geometry, low number of observations) the results are well within our expectations. Taking into account the low accuracy of the used orbit data, also the estimated orbit offsets meet our expectations — with the largest component (-7.8 m) in the along-track direction.

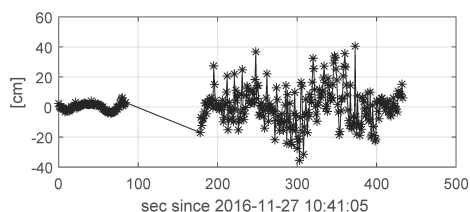


Fig. 4 Post-fit residuals of Scans 168 and 169 in Experiment a332.

Table 2 Estimation results from Scans 168 and 169 in Experiment a332.

Parameter	Estimates	Formal Errors
Clock offset, Hb	14.0 m	2.3 m
Clock offset, Ke	-1.1 m	1.9 m
ZWD, Hb	3.4 cm	1.7 cm
ZWD, Ke	14.3 cm	2.1 cm
ZWD, Yg	7.3 cm	1.7 cm
Orbit, radial	1.2 m	0.3 m
Orbit, along-track	-7.8 m	0.3 m
Orbit, cross-track	-1.9 m	1.3 m

6 Summary and Discussion

This paper describes a series of VLBI observations of the APOD-A nano satellite performed in November 2016 by the AuScope geodetic VLBI array. Although the observations were extremely challenging — mainly due to the low orbit of the satellite and its high speed — we were able to derive results in terms of OMC residuals on the nanosecond level. While the observations are still not sufficient to be used for actual frame tie studies, a simple test case proved that the parameter estimation in VieVS based on such data in principle works.

This case study also revealed some limitations. The available observation geometry (intra-continental baselines and the low orbit, see Figure 1) only allowed observing of a few single baseline scans per day. Hence, a denser tracking network would be needed to increase the number of observations. Furthermore, globally distributed tracking stations are a prerequisite to estimate reliable orbit parameters, as they would allow observing full orbit arcs.

For more details on this case study the authors refer to Hellerschmied et al. (2018).

Acknowledgements

This study made use of the AuScope VLBI infrastructure. It was supported by the Austrian Science Fund (FWF, projects SORTS I2204 and J3699-N29) and by the National Natural Science Foundation of China (Grant No. 11603001). We thank the Vienna Scientific Cluster (VSC-3) for supporting our VLBI work.

References

- Alizadeh MM, Wijaya DD, Hobiger T, Weber R, Schuh H (2013) Ionospheric Effects on Microwave Signals. In: Böhm J, Schuh H (eds) *Atmospheric Effects in Space Geodesy*, Springer Berlin Heidelberg, Berlin, Heidelberg, 35–71, DOI 10.1007/978-3-642-36932-2_2
- Altamimi Z, Rebischung P, Métivier L, Collilieux X (2016) ITRF2014: A new release of the International Terrestrial Reference Frame modeling non-linear station motions. *Journal of Geophysical Research: Solid Earth* 121(8):6109–6131, DOI 10.1002/2016JB013098
- Biancale A, Pollet A, Coulot D, Mandea M (2017) E-GRASP/Eratosthenes: a mission proposal for millimetric TRF realization. In: *Conference Abstracts of the 19th EGU General Assembly*, p 8752
- Böhm J, Böhm S, Boisits J, Girdiuk A, Gruber J, Hellerschmied A, Krásná H, Landskron D, Madzak M, Mayer D, McCallum J, McCallum L, Schartner M, Teke K (2018) Vienna VLBI and Satellite Software (VieVS) for Geodesy and Astrometry. *Publications of the Astronomical Society of the Pacific* 130(986), DOI 10.1088/1538-3873/aaa22b
- Deller AT, Brisken WF, Phillips CJ, Morgan J, Alef W, Cappallo R, Middelberg E, Romney J, Rottmann H, Tingay SJ, Wayth R (2011) DiFX-2: A More Flexible, Efficient, Robust, and Powerful Software Correlator. *Publications of the Astronomical Society of the Pacific* 123(901):275, DOI:10.1086/658907.
- Haas R, Hobiger T, Klotek G, Kareinen N, Yang J, Combrinck L, de Witt A, Nickola M (2017) VLBI with GNSS-signals on an Intercontinental Baseline – A progress report. In: Haas R, Elgered G (eds) *Proceedings of the 23rd European VLBI Group for Geodesy and Astrometry Working Meeting*, May, 2017, Gothenburg, Sweden, 117–121
- Hellerschmied A, Plank L, Neidhardt A, Haas R, Böhm J, Plötz C, Kodet J (2014) Observing satellites with VLBI radio telescopes - practical realization at Wettzell. In: Behrend D, Baver K, Armstrong K (eds) *IVS 2014 General Meeting Proceedings - "VGOS: The New VLBI Network"*, Science Press, 441–445
- Hellerschmied A, Böhm J, Neidhardt A, Kodet J, Haas R, Plank L (2017) Scheduling VLBI Observations to Satellites with VieVS. In: van Dam T (ed) REFAG 2014: Proceedings of the IAG Commission 1 Symposium Kirchberg, Luxembourg, 13–17 October, 2014, Springer International Publishing, 59–64, DOI 10.1007/1345_2015_183
- Hellerschmied A, McCallum L, McCallum J, Sun J, Böhm J, Cao J (2018) Observing APOD with the AuScope VLBI Array. *Sensors* 18(5), DOI 10.3390/s18051587
- Klioner S (1991) General Relativistic Model of VLBI Observables. In: Alef W, Bernhart S, Nothnagel A (eds) *Proceedings of the AGU Chapman Conference on Geodetic VLBI: Monitoring Global Change*, Washington D.C., April 22–26, 1991, NOAA Technical Report NOS 137 NGS 49, 188–202
- Lovell JEJ, McCallum JN, Reid PB, McCulloch PM, Baynes BE, Dickey JM, Shabala SS, Watson CS, Titov O, Ruddick R, Twilley R, Reynolds C, Tingay SJ, Shield P, Adada R, Ellingsen SP, Morgan JS, Bignall HE (2013) The AuScope geodetic VLBI array. *Journal of Geodesy* 87(6):527–538, DOI 10.1007/s00190-013-0626-3
- Nerem RS, Draper RW (2011) Geodetic Reference Antenna in Space. GRASP proposal submitted in response to NNH11ZDA0120 prepared for National Aeronautics and Space Administration Science Mission Directorate September 29, 2011
- Plank L, Hellerschmied A, McCallum J, Böhm J, Lovell J (2017) VLBI observations of GNSS-satellites: from scheduling to analysis. *Journal of Geodesy* 91(7):867–880, DOI 10.1007/s00190-016-0992-8
- Sun J, Tang G, Shu F, Li X, Liu S, Cao J, Hellerschmied A, Böhm J, McCallum L, McCallum J, Lovell J, Haas R, Neidhardt A, Lu W, Han S, Ren T, Chen L, Wang M, Ping J (2018) VLBI observations to the APOD satellite. *Advances in Space Research* 61(3):823–829, DOI {10.1016/j.asr.2017.10.046}
- Tornatore V, Haas R, Casey S, Pogrebenko S, Molera Calvés G (2014) Direct VLBI Observations of Global Navigation Satellite System Signals. In: Rizzos C, Willis P (eds) *Earth on the Edge: Science for a Sustainable Planet*, Proc. IAG General Assembly, 2011, Springer Berlin Heidelberg, International Association of Geodesy Symposia, vol 6, 247–252